Progress in Medical Devices
eISSN: 2957-5478

Zentime

Review Article https://doi.org/10.61189/594641kmfbkw

A method for identifying pleural lines in B-mode ultrasound images

Tingting Zhou[1], Haozhe Zhuang[1], Shiju Yan[1], Erze Xie[1], Yibo Ma[2], Tao Zhang[1], Tianxiang Yu[1], Shuang Deng[1]

[1]School of Health Science and Engineering, University of Shanghai for Science and Technology, Shanghai 200093, China. [2]Department of Ultrasound, the Third Affiliated Hospital of Soochow University, Changzhou 213000, Jiangsu, China.

Declaration of conflict of interest: None.

Received March 17, 2023; Accepted August 28, 2023; Published September 30, 2023

Highlights

- Automated pleural line identification: A method was introduced to automatically identify pleural lines in lung ultrasound images, ensuring diagnosis speed and accuracy.
- High reliability: An average of 90.45% identification rate of pleural lines was achieved in a comprehensive experiment on 890 ultrasound videos, highlighting its broad applicability and reliability.
- Efficient integration: The algorithm's rapid processing (1.36 seconds for a 5-second video) makes it suitable for seamless integration into ultrasound instrument software, aiding clinicians in diagnosing conditions like pneumothorax more efficiently.

Abstract

In ultrasound imaging, the pleura is visualized as echo reflection formed by the echoes of the interface between the pleura and the lung surface. Three major signs of pleura determines whether the patient has pneumothorax. In this paper, we propose a method to identify pleural line for the diagnosis of pneumothorax. Firstly, the gray threshold of ultrasonic image is properly classified by pre-experiment. Secondly, possible pleural line regions are identified based on threshold classification. Thirdly, the region of pleural line is identified based on the known characteristics of pleural line. The last step is to consider whether it is necessary to modify the threshold to accurately identify the pleural line region. Moreover, we tested 890 ultrasound samples, which included three categories: lung sliding, lung point, and lung sliding disappearance. Each category of samples was divided into two subsets, typical and atypical. The average identification rate reached 90.45%. According to the test results, the advantages and disadvantages of the proposed method as well as the further improvement direction were analyzed. This method for identifying pleural line can serve as the groundwork for developing automatic algorithm for diagnosing pneumothorax.

Keywords: Pleural line identification, lung ultrasound, pneumothorax, automatic identification algorithm, image processing

Introduction

The pleura is a thin, smooth serous membrane adhering to the inner chest wall and the lung surface. In ultrasound images, the pleura, also known as the pleura line, is presented as echo reflection formed by the echoes of the interface between the pleura and the lung surface. Serving as a key anatomical marker, the pleural line plays an important role in chest ultrasound, and it is the basis for the evaluation of several basic signs in chest ultrasound, such as pleural sliding sign, seashore sign, stratospheric sign, A-lines, and B-lines. Disappearance of pleural line and static, rough, thickened or irregular pleural line are all abnormal signs [1, 2]. The pleural line is associated with the diagnosis and interventional treatment of many pulmonary diseases, such as pneumothorax, pulmonary atelectasis, pleural effusion, pleural hemorrhage, pleural tumor, and ultrasound-guided thoracic drainage [3, 4]. Especially in the diagnosis of pneumothorax, the identification of pleural line plays a key role [1-4].

In ultrasound diagnosis of pneumothorax, there

Address correspondence to: Shiju Yan, School of Health Science and Engineering, University of Shanghai for Sci-ence and Technology, No.516 Jungong Road, Shanghai 200093, China. Email: yanshiju@usst.edu.cn; **Yibo Ma**, Department of Ultrasound, the Third Affiliated Hospital of Soochow University, No.185 Juqian Street, Changzhou 213000, Jiangsu, China. Email: mayibo@czfph.com.

are mainly three signs of pleural line: (1) complete presence of lung sliding, namely normal pleural sliding sign, which shows that the pleura moves with breathing; (2) partial presence of lung sliding, which is characterized by partial movement of the pleura, and the junction of pneumothorax with and without lung sliding is lung point; (3) disappearance of lung sliding, namely abnormal pleural sliding sign, which shows that the pleura does not move. The above signs are the main basis for the diagnosis of pneumothorax. The evaluation of pleural sliding sign and lung point sign is based on the accurate identification of pleural line [1, 2, 5-9]. Therefore, identifying the pleural line is of great significance in the ultrasonic diagnosis of pneumothorax.

At present, the identification of pleural lines mainly relies on the clinicians' observation and experience, which leads to certain limitations [10-12]. (1) Inexperienced clinicians may easily mistake the pleural line for myofascial or the interface between muscle and adipose layer. (2) Some pleural lines may exhibit irregular shapes in ultrasonic examinations, leading to a time-consuming identification process that demands experienced clinicians for accurate recognition. (3) Using manual observational methods to identify pleural line lacks objectivity. Automatic pleural line identification can detect the position of pleural line quickly and quantitatively without the use of human labor. The results can be applied not only for pneumothorax diagnosis but also for intelligent diagnosis of other pulmonary diseases.

A number of intelligent algorithms have been developed for automatic pleural line identification. Moshavegh et al. used the random walk-based segmentation method proposed by Grady to compute confidence map. The pleural line is delineated on the confidence map by thresholding the confidence map to be higher than the global threshold of the entire map [13, 14]. Anantrasirichai et al. proposed a linear restoration method of speckle image [15]. Based on Radon transform and sparse regularization, the linear pleural line can be accurately extracted. However, this method still has limitations in identifying irregular pleural lines. Furthermore, Chen et al. proposed an automatic pleural line identification method based on Radon transform [16]; however, this method is limited to the use of ultrasound video for verification, and the effect of identifying pleural lines for videos not within this range is unknown. Carrer et al. proposed an automatic pleural line identification algorithm based on hidden Markov model and Viterbi algorithm [17]. The algorithm can be used to accurately extract the pleural lines in most videos, but it still misestimates the gray threshold of some ultrasound images with low contrast. The above-mentioned traditional algorithms still have a long way to further improve the accuracy. Although the accuracy of neural network and other machine learning algorithms is significantly better than that of traditional algorithms, such as the identification of abnormalities in ultrasound lung images proposed by Veeramani, machine learning algorithms still need a lot of data training to ensure their accuracy [18-20]. However, medical related resources are limited and private, so it is difficult to obtain data. Therefore, it is still necessary to study the traditional algorithms to further improve the pleural line identification rate. In this study, we analyzed and compared the pleural lines in B-mode ultrasound videos of pneumothorax patients and non-pneumothorax patients. Based on the characteristics of linear strong echo in ultrasonic identification of pleural line, an automatic identification algorithm for pleural line in pneumothorax diagnosis is proposed in order to improve the accuracy of pleural line identification, so as to improve the work efficiency of clinicians and the accuracy and efficiency of diagnosis.

Methods

The gray threshold was determined to be 100 by pre-experiments. Based on the area S with pixel gray values greater than 100 in the gray histogram of an ultrasound video, the gray threshold Y of the pleural line area was determined, which was taken as a variable that could be adjusted. Because the pleural line is smooth, uniform and linear with high echo, the correct pleural line region can be extracted based on this characteristic. The adequacy of the threshold value can be evaluated by calculating the extracted pleural line area, thereby determining whether any adjustments to the threshold value are necessary. This process establishes a closed loop of identification system, thereby extracting the correct pleural line region. A flowchart of the proposed pleural line identification method is shown in **Figure 1**.

Threshold classification

In ultrasound videos, pleural lines usually have high brightness (gray value) due to differences in acoustic impedance between the pleura and the lung surface interface. Theoretically, as long as the appropriate gray threshold is set, the pleural line regions in ultrasound video can be separated and extracted. Nevertheless, in practice due to different ultrasonic equipment,

Table 1. Gray threshold classification

Area S	S≤90k	90k<S≤150k	150k<S≤400k	400k<S
Gray threshold *y*	120	150	160	210

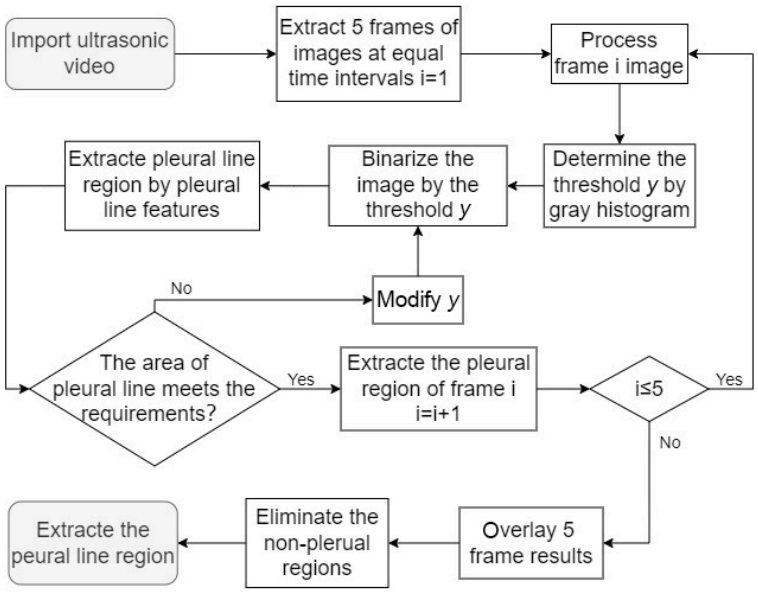

Figure 1. Flowchart of pleural line identification.

diagnostic frequency and other factors, it is impossible to set one gray threshold applicable to all videos, as shown in **Figure 2**. Therefore, before the extraction of pleural line area, it is necessary to carry out a regular threshold classification, so that specific gray thresholds can be set for target videos to extract pleural line. Particularly, the threshold classification is not based on biophysical basis, but on the global gray value of the images.

Results of pre-experiments showed that the area with pixel values larger than the threshold was positively correlated with the selected threshold. The larger the area in which pixel values exceed the threshold, the larger the bright line's area in the image, necessitating the setting of a higher gray threshold. By observing gray histograms of different videos, it was found that the pixel value threshold of 100 was proper for extracting regions incorporating pleural lines, so the threshold of 100 was set as the classification standard. Based on this threshold, the regions with pixel values greater than 100 were obtained, and the pixel value thresholds were classified. The classification results are shown in **Table 1**. Additionally, the threshold was slightly larger so that the area would be slightly smaller, simplifying subsequent steps, where the focus is on determining whether to decrease the threshold instead of increasing it.

Pleural line extraction

In the algorithm of automatic pleural line identification, 5 frames were extracted from each 5-second ultrasonic video at equal intervals, and the 5 frames were superimposed into one image. The purpose of this operation was to avoid the disappearance or blurring of pleural lines in a few frames of 5-second ultrasound videos. Then, regions with pixel values greater than 100 were extracted, and the gray threshold was classified based on areas of these regions, as shown in **Table 1**.

Then each frame of a 5-second ultrasonic video was processed as follows.

Step 1: Process the initial image (**Figure 3A**) as follows. Obtain the binary image. The gray value greater than the initial threshold *y* was set to 1, and the gray value less than the threshold *y* was set to 0. All connected regions were extracted with pixel values greater than the gray threshold *y* (**Figure 3B**). Then, the threshold *y* was adjusted according to all the connected areas and the relationship between the area and the threshold obtained in **Table 1**. As shown in **Figure 3C**, the binary graph was extracted based on the modified threshold *y*.

Step 2: Remove the non-pleural line regions. The noise regions were deleted according to their small areas, and the attribute set of the remaining regions were obtained. The attribute set contained the measured values of several attributes of each 8-connected object in the binary image, including the center of mass and the range of the horizontal and vertical coordinates of the region. Only the potential pleural line area was left (**Figure 3D**).

Step 3: Extract the pleural line based on the characteristics. The pleural line is usually long and almost runs through the whole frame width. Moreover, the pleural line is always located at a moderate height of the image. Ac-

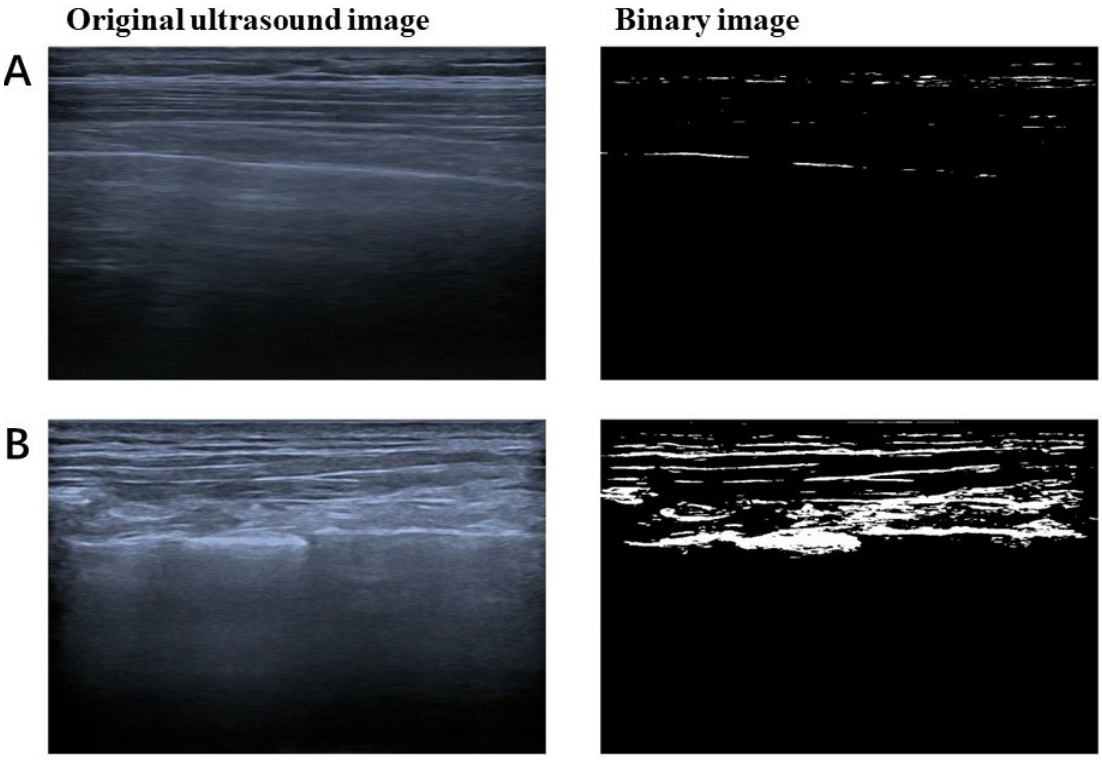

Figure 2. Threshold classification explanatory figure. The gray threshold for both figures were set to be the same, making it impossible to accurately separate the pleural line later. (A) The pleural line is incompletely extracted due to the too high threshold (under segmentation); (B) Other highlighted areas adhering to pleural line area are extracted as pleural line due to the too low threshold (over segmentation).

cording to the characteristics of pleura line, the values of the upper and lower fifths of the binary image were set to 0, which could exclude the regions with very low possibility of pleura line. Referring to the attribute set obtained from step 2, the regions with transverse lengths less than two-fifths of the image width were excluded. Because the muscular fascia above the pleural line usually has a high gray value, the lowest connected region is preliminarily determined as the pleural line region. The area of this region was calculated to determine whether it belonged to pleural line. If the area is too small, the threshold value must be too high. Then, the threshold value was reduced by 20 to repeat the above two steps (**Figure 3E**).

Step 4: Superimpose the results of the 5 frames of binary images on one image. As shown in **Figure 4A**, the darker the color, the more likely this region is to be a pleural line region. The region with lighter color is the movement of pleural line in the direction of non-pleural line caused by factors such as probe instability, which should be eliminated. In the superimposed image, only a superimposed value greater than 2 was left. Finally, the connected component with the largest area was determined as the pleural line region (**Figure 4B**).

Experiments

Materials

Imaging samples used in this study were all from the Department of Ultrasound of the Third People's Hospital Affiliated to Soochow University. SONIMAGE HS1color ultrasound diagnostic instrument of Konica Minolta was used for ultrasonic examinations, with a probe frequency of 4-18 mhz. During ultrasonic examinations, the subjects were in supine or sitting position. The second intercostal longitudinal section of the central clavicular line and the transverse section of the intercostal space were taken as the routine sections, and the ultrasonic probe was placed perpendicular to the patient's skin during the examinations. The machine was adjusted so that the pleura could be clearly displayed. Video acquisition, pleural line identification, annotation, typical or atypical judgment, and pneumothorax diagnosis were all performed by clinicians with more than 5 years of experience in ultrasound diagnosis. These samples cover three categories: lung sliding, lung point, and lung sliding disappearance. Each category of samples was divided into two

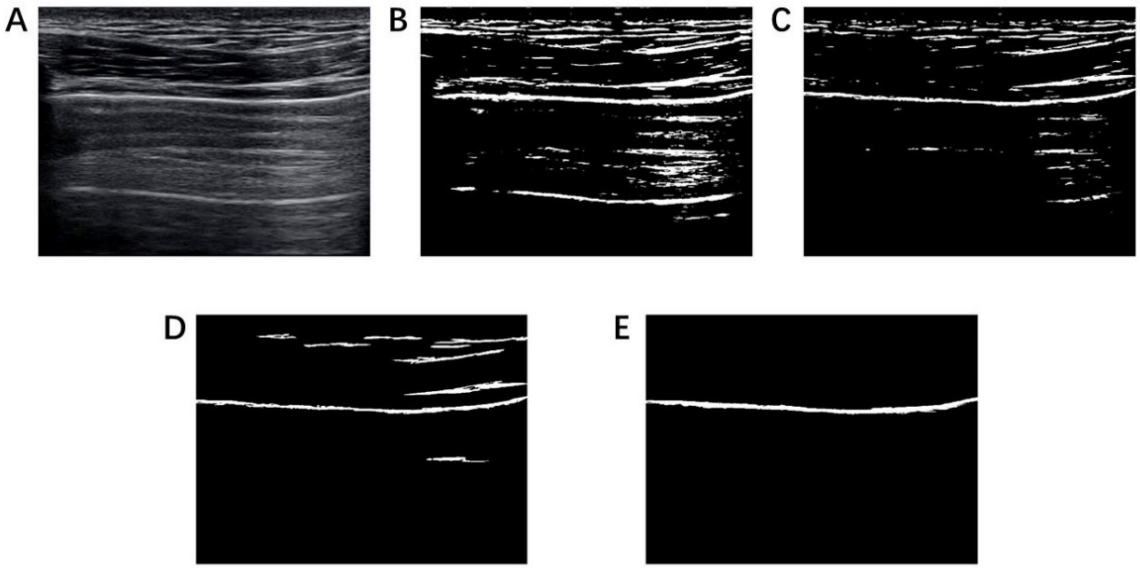

Figure 3. Illustration of pleural line extraction process. (A) Original image; (B) Binary image; (C) Binary image based on *y*; (D) Image of possible pleural line; (E) Image of recognized pleural line.

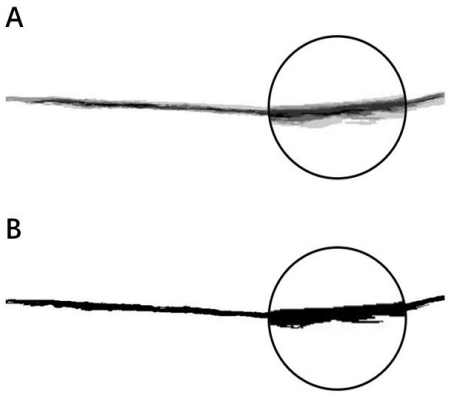

Figure 4. Processed diagram of stacking results (The inside circle is the enlarged image). (A) Superimposing the images; (B) Result image after removing regions generated by motion.

subsets, typical and atypical, according to the significance of signs determined by ultrasound clinicians. A total of 890 5-second B-mode lung ultrasound videos were collected, including 261 lung sliding videos, 331 lung point videos, 298 lung sliding disappearing videos. The 890 videos included 715 typical ones and 175 atypical ones. The study was approved by the Ethics Committee of Changzhou First People's Hospital. All patients provided written informed consents. The study is retrospective.

Experiments

In order to verify the performance of the proposed pleural line identification method, clinicians with over 5 years of experience in ultrasound diagnosis tried to identify the pleural line using this method. The clinicians manually delineated the pleural line area on the superimposed image, as shown in **Figure 5A**. The image delineated by the clinicians was saved as a binary image, and the delineated region was set as the gold standard of the pleural line region, with ±10 pixels as the allowable error range. In **Figure 5B**, the black region is the delineated region, and the gray region is the allowable error range. The image was used as the gold standard for determining the position of the pleural line in the corresponding 5-second ultrasound video. The pleural line region image obtained by the proposed pleural line identification method was compared with the gold standard. Within the allowable range of error, a 95% agreement was found between the proposed method and the gold standard.

Results

A total of 890 ultrasound videos were analyzed by the proposed pleural line identification method in 1,212.62 seconds, and the pleural lines of 805 ultrasound videos were identified correctly. The average identification rate reached 90.45%. The detailed identification rates of pleural lines in various ultrasound videos are shown in **Figure 6**. The identification success rate of each category was calculated by the formula: success recognition rate = number of successful recognition times / total number of samples under this classification * 100%.

Discussion

The results of this study indicate that the proposed identification method exhibits good accu-

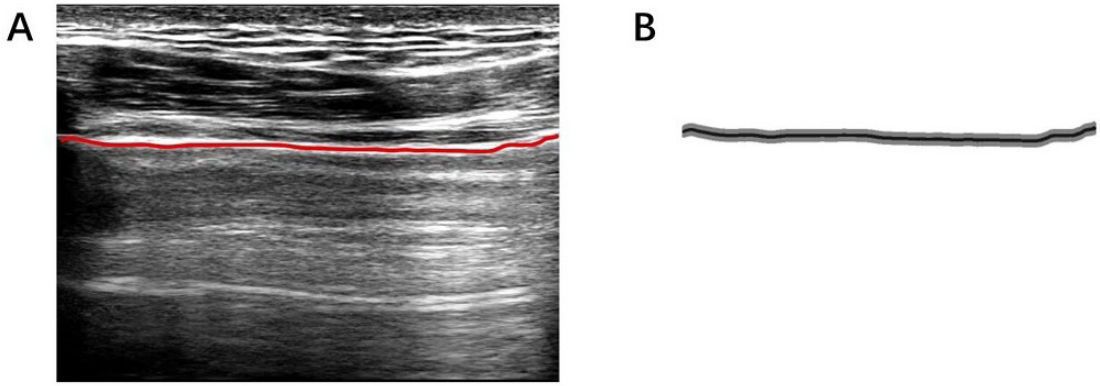

Figure 5. Pleural line obtained by gold standard. (A) The clinician manually outlined the pleural line. (B) The final pleural line as gold standard.

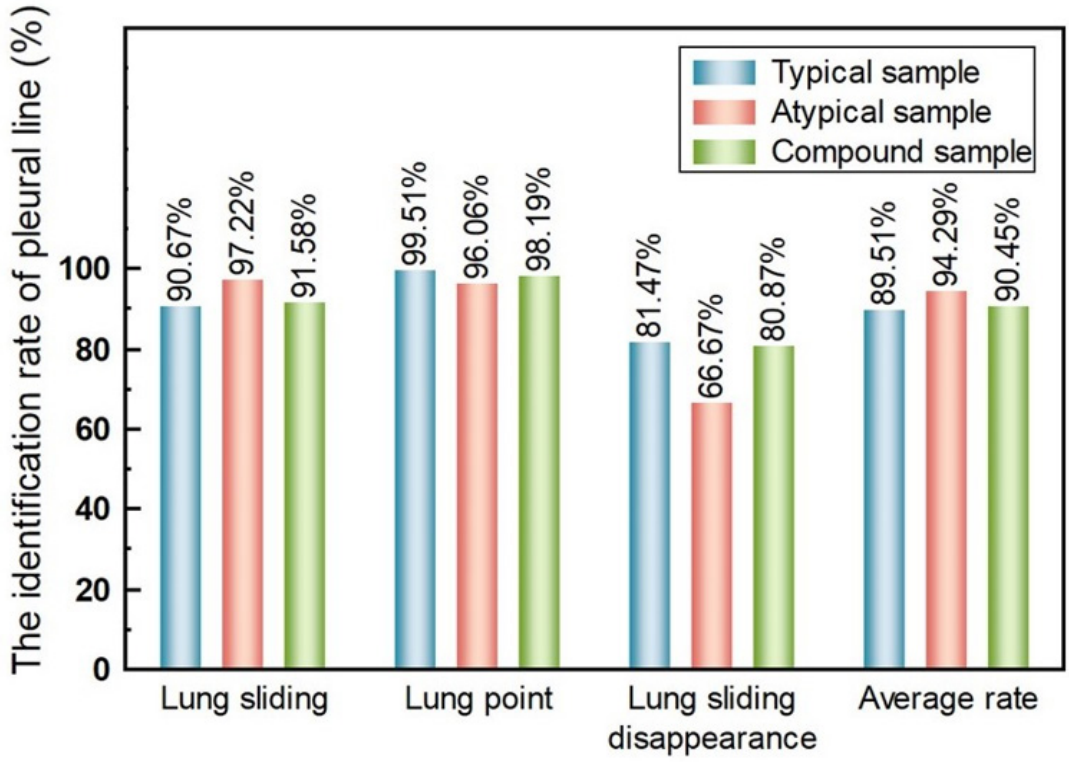

Figure 6. The identification rate of pleural line.

racy, universality and reliability. (1) The pleural line region identified by the proposed method and the pleural line delineated by the clinicians had an agreement of over 95%, indicating the high accuracy of the proposed method. (2) In general, the method has a good identification rate for the videos with lung sliding and lung point, but the identification rate of lung sliding disappearance video was 80.87%, which is lower than the average identification rate of 90.45%. That is, the method can better identify the pleura line in cases of lung sliding and lung point, with a certain universality. (3) When testing the typical and atypical ultrasound videos, there was a difference in the identification rate between typical and atypical ultrasound videos in the category of lung sliding disappearance, which may be caused by the small number of atypical test sets. However, with a larger number in the atypical subsets, there were no significant differences in the identification rate of pleura line between typical and atypical ultrasound videos in the categories of lung sliding and lung point. Generally, the algorithm has a certain reliability.

The identification rate of the pleural lines in the ultrasound videos with the disappearance of lung sliding is slightly lower. This may be attributed to the absence of lung sliding, because long and bright linear strong echo lines are often associated with the pleural line. This echo line looks very similar to the pleura line, so the method is prone to misjudgment (**Figure 7A**).

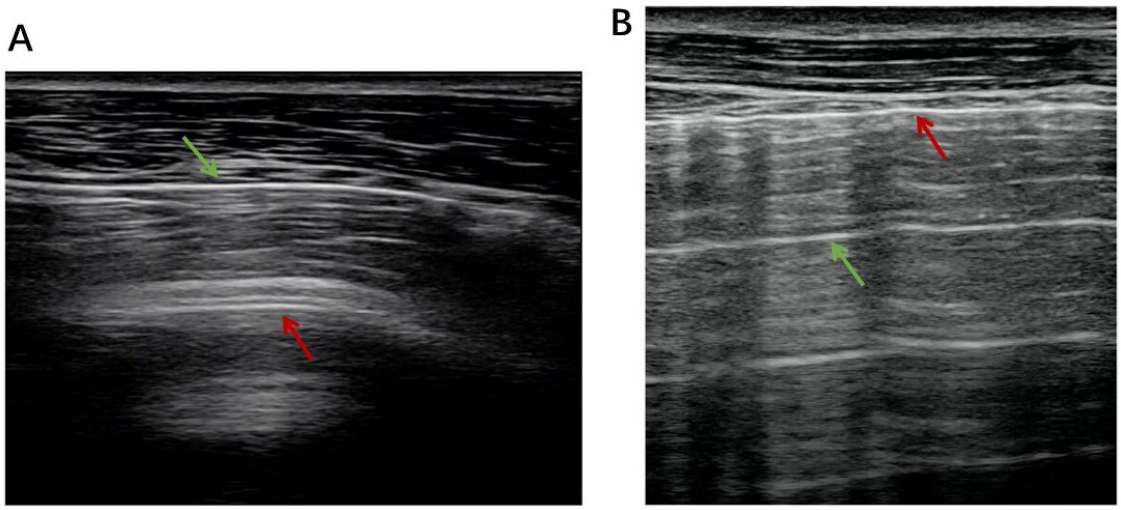

Figure 7. Wrong identification of pleural line. The green arrows point to the correct pleural line area, and the red arrows point to the wrongly identified pleural line area. (A) Error condition 1; (B) Error condition 2.

However, there were only 12 ultrasound videos of atypical lung sliding disappearance, so the results with low recognition rate may not be representative. Besides, the identification rate of pleural lines in ultrasound videos of lung sliding was slightly low than that of lung point. This may be due to the fact that some flow point on the pleural line diluted the highlighted state of the pleural line during lung sliding. It may also be related to equipment, frequency and other factors, resulting in unclear pleural lines in some videos, making the identification more difficult. Pleura line is then mistakenly identified as muscle fiber, myofascial membrane and other tissues with high gray values in ultrasound, as shown in **Figure 7B**. In general, the identification rate of typical videos was even slightly lower than that of atypical videos, which means whether the sign is typical has little influence on the identification performance of the proposed pleural line identification method.

In a clinical context, clinicians require extensive experience and advanced skills to accurately identify pleural lines. The proposed method can be used to identify pleural lines accurately and rapidly, thus improving the diagnostic efficiency and reducing eye fatigue. The method proposed in this paper can assist clinicians lack of clinical experience to identify pleural lines, and at the same time accumulate experience and improve confidence. However, the identification rate of the method is not very high in cases of lung sliding disappearance, so a secondary manual identification may be needed for this type of video in clinical use.

The method described in this paper provides a basis for the research on automatic diagnosis of pneumothorax and other pleural diseases. Accurate identification of pleural lines can enhance the diagnosis efficiency of pleural diseases such as pneumothorax, pleural effusion, pleural bleeding, and pleural tumor.

However, there are still some limitations in this method. There are only a few atypical samples in case of lung sliding and disappearance of lung sliding, so more clinical data are needed to verify the performance of the proposed method. The identification rate of pleura line in case of lung sliding disappearance is low, so the algorithm needs to be further improved. For example, by learning more about the characteristics of the pleura lines, more precise rules can be set for the extraction of pleura line.

In our future research, we will combine more clinical applications and data to comprehensively verify the universality of the proposed algorithm and improve its identification rate. Meanwhile, the algorithm will be integrated into the software system of the ultrasound mainframe to form an automatic recognition module for pleural lines. This will enable the ultrasound device to automatically or manually activate this module, to facilitating automatic recognition of pleural line.

Conclusion

In pulmonary ultrasound, the identification of pleural line is the most basic and important. This paper presents an automatic pleural line identification method for the diagnosis of pneumothorax. The algorithm realizes fast and accurate automatic identification of pleural line regions in ultrasound videos by proper gray threshold classification based on the high brightness of pleural lines in ultrasound

videos. In the verification experiment using 890 ultrasound videos of three categories, the results showed that the average identification rate of pleural lines was 90.45%, which verifies the universality and reliability of the proposed method. The algorithm took an average of 1.36 seconds to process a 5-second ultrasound video, proving its fast speed. As a means to assist clinicians to detect pleural line, it can be integrated into the software system of ultrasound instruments to reduce the pressure of clinicians and improve the diagnosis efficiency of diseases such as pneumothorax.

References

[1] Gargani L. Ultrasound of the Lungs: More than a Room with a View. Heart Fail Clin 2019;15(2):297-303.

[2] Wangüemert Pérez AL. Clinical applications of pulmonary ultrasound. Med Clin (Barc) 2020;154(7):260-68.

[3] Wernecke K. Ultrasound study of the pleura. Eur Radiol 2000;10(10):1515-23.

[4] McLoud TC, Flower CD. Imaging the pleura: sonography, CT, and MR imaging. Am J Roentgenol 1991;156(6):1145-53.

[5] Salah AI, El-Serwi HBe-D, Ansary AMA, et al. Pleural ultrasonography versus chest radiography for the diagnosis of pneumothorax. QJM-INT J MED 2021;114(Supplement_1).

[6] Ramos HC, Núñez DM, Botana RM, et al. Validity of lung ultrasound to rule out iatrogenic pneumothorax performed by pulmonologists without experience in this procedure. Rev Clin Esp 2021;221(5):258-63.

[7] Soldati G, Demi M, Smargiassi A, et al. The role of ultrasound lung artifacts in the diagnosis of respiratory diseases. Expert Rev Resp Med 2019;13(2):163-72.

[8] Luna G, Marica D, Luigia D, et al. Ultrasound lung comets in systemic sclerosis: a chest sonography hallmark of pulmonary interstitial fibrosis. Rheumatology 2009;48(11):1382-87.

[9] Mearelli F, Casarsa C, Trapani A, et al. Lung ultrasound may support internal medicine physicians in predicting the diagnosis, bacterial etiology and favorable outcome of community-acquired pneumonia. Sci Rep 2021;11(1):17016.

[10] Marchetti G, Arondi S, Baglivo F, et al. New insights in the use of pleural ultrasonography for diagnosis and treatment of pleural disease. Clin Respir J 2018;12(6):1993-2005.

[11] Anderson KL, Fields JM, Panebianco NL, et al. Inter-Rater Reliability of Quantifying Pleural B-Lines Using Multiple Counting Methods. J Ultras Med 2013;32(1):115-20.

[12] Koenig SJ, Narasimhan M, Mayo PH. Thoracic Ultrasonography for the Pulmonary Specialist. CHEST. 2011;140(5):1332-41.

[13] Moshavegh R, Hansen KL, Sorensen HM, et al. Novel automatic detection of pleura and B-lines (comet-tail artifacts) on in vivo lung ultrasound scans. SPIE 2016;9790:1-7.

[14] Grady L. Random walks for image segmentation. IEEE T Pattern Anal 2006;28(11):1768-83.

[15] Anantrasirichai N, Hayes W, Allinovi M, et al. Line detection as an inverse problem: application to lung ultrasound imaging. IEEE T Med Imaging 2017;36(10):2045-56.

[16] Chen J, Li J, He C, et al. Automated pleural line detection based on radon transform using ultrasound. Ultrasonic Imaging 2021;43(1):19-28.

[17] Carrer L, Donini E, Marinelli D, et al. Automatic pleural line extraction and COVID-19 scoring from lung ultrasound data. IEEE T Ultrason Ferr 2020;67(11):2207-17.

[18] Roy S, Menapace W, Oei S, et al. Deep Learning for Classification and Localization of COVID-19 Markers in Point-of-Care Lung Ultrasound. IEEE T Med Imaging 2020;39(8):2676-87.

[19] Wu Y, Yi Z. Automated detection of kidney abnormalities using multi-feature fusion convolutional neural networks. Knowl-Based Sys 2020;200:105873.

[20] Veeramani SK, Muthusamy E. Detection of abnormalities in ultrasound lung image using multi-level RVM classification. J Matern-Fetal Neo M 2016;29(11):1844-52.